

On the comparison of heterogeneous mechanical tests for sheet metal characterization

GONÇALVES Mafalda^{1,a,*}, OLIVEIRA Miguel Guimarães^{1,2,b},
THUILLIER Sandrine^{2,c} and ANDRADE-CAMPOS António^{1,d}

¹Centre for Mechanical Technology and Automation (TEMA), LASI – Intelligent Systems Associate Laboratory, Department of Mechanical Engineering, University of Aveiro, Portugal

²Univ. Bretagne Sud, UMR CNRS, IRDL, F-56100 Lorient, France

^amafalda.goncalves@ua.pt, ^boliveiramiguel@ua.pt, ^csandrine.thuillier@univ-ub.fr, ^dgilac@ua.pt

Keywords: Heterogeneous Tests, KPIs, Material Behavior, Sheet Metal

Abstract. The characterization of sheet metal behavior is of utmost importance for the accurate virtualization of sheet metal forming processes. Newly proposed mechanical testing approaches are overcoming the use of standard mechanical tests. Test configurations with more complex geometries present richer mechanical fields and, therefore, provide a higher quantity of valuable information about the material behavior in a more efficient manner. To extract that information, full-field measurement techniques such as Digital Image Correlation are being used. Although several test designs have already been proposed, the choice of the best one to calibrate a chosen mechanical model is still an issue. This work aims at proposing Key Performance Indicators (KPIs) that are able to rank mechanical tests by their potential to enhance the material behavior characterization process. These metrics evaluate quantitatively the quality and the importance of the data that each test can provide. The potential of three test designs to characterize accurately sheet metal mechanical behavior is analyzed using the proposed KPIs. From a uniaxial tensile loading test up to rupture, the numerical mechanical information is extracted, and the performance of each test is evaluated and compared.

Introduction

Sheet metal forming processes play a major role in the development of mechanical parts for several industries such as automotive and aircraft. The virtualization of these processes has gained wide popularity in the transition to a more sustainable industry. Reduced costs, time, and material waste associated with the experimental task can be achieved. However, an accurate digitalization of the forming process is only possible when the numerical model can represent reality. For instance, the material constitutive model chosen to define the material behavior has to be well calibrated, having a huge repercussion on the obtained results. A classical model calibration procedure demands a huge quantity of data from several standard mechanical tests. The time and costs associated with this task led to the emergence of new ways of mechanical testing. The so-called heterogeneous testing consists in test configurations that have the potential to provide a significant amount of data with just a single test. Whether they present more complex boundary conditions or geometries, heterogeneities in the mechanical fields are induced, leading to a more informative test.

Several innovative designs have already been proposed to overcome the standardized mechanical testing. The design process of these tests has been led mainly by two approaches searching for: (i) the heterogeneity of the mechanical fields that are induced on the specimen [1–7] and (ii) the quality of the material model parameters that are identified [8–11]. A more comprehensive review of the mechanical tests commonly used for material characterization and model calibration can be found in [14].

The use of heterogeneous mechanical tests is only achievable due to the emergence of full-field measurement techniques, such as Digital Image Correlation [15]. As an optical technique, it has

the ability to extract information about the strain fields at each material point. Therefore, a larger quantity of information can be extracted from one heterogeneous test using full-fields techniques. With this data, it is possible to calibrate material constitutive models more efficiently using inverse methodologies such as the Finite Element Model Updating (FEMU) technique [16] and the Virtual Fields Method (VFM) [17]. The quality of the identification depends on the quality of the mechanical information that can be retrieved from the specimen. For instance, the heterogeneity of the mechanical fields, the magnitude and distribution of the equivalent plastic strain and the sensitivity of the induced fields to the parameters to be identified are aspects that have a huge influence on the identification quality.

Several designs of tests have been proposed with the aim of trying to characterize material behavior more accurately and cost-effectively. However, it is still unclear how to choose the best test geometry to calibrate a chosen material model. The choice of the most suitable test is not straightforward, so appropriate metrics should be established to evaluate and compare the performance of each test in the model calibration and material identification procedures.

This work aims at filling this gap and establishing Key Performance Indicators (KPIs) that analyze the potential of each test design to provide valuable data for the material characterization and model calibration procedures. Three heterogeneous tests, deformed up to rupture under a uniaxial load, were chosen to be analyzed. The investigation is in a first step purely numerical. Based on the mechanical fields, the potential of each test was evaluated using the proposed KPIs.

Heterogeneous Tests Analysis

Key Performance Indicators. The aim of this work consists in evaluating and comparing the potential of each test to provide relevant information for the material identification and model calibration procedures. For that, some scalar metrics are here proposed. The first metric consists in a mechanical indicator proposed by Souto et. al. [12] that can be defined as

$$I_T = w_{r1} \frac{\text{Std}(\varepsilon_2/\varepsilon_1)}{w_{a1}} + w_{r2} \frac{(\varepsilon_2/\varepsilon_1)_R}{w_{a2}} + w_{r3} \frac{\text{Std}(\bar{\varepsilon}^p)}{w_{a3}} + w_{r4} \frac{\bar{\varepsilon}_{\max}^p}{w_{a4}} + w_{r5} \frac{\text{Av}(\bar{\varepsilon}^p)}{w_{a5}}, \quad (1)$$

where ε_1 and ε_2 are the principal major and minor strains in the sheet plane, respectively. The equivalent plastic strain, $\bar{\varepsilon}^p$, and its maximum value, $\bar{\varepsilon}_{\max}^p$, are also considered as evaluation criteria for the test. This indicator evaluates different features: the strain state standard deviation, the strain state range, the standard deviation, the maximum, and the average value of the equivalent plastic strain. The importance of each term is adjusted and normalized using absolute values (w_{ai} , with $i \in [1,5]$) and relative weights (w_{ri} , with $i \in [1,5]$). The chosen values for these parameters can be seen in Table 1. A more detailed description of the indicator as well as the established values for the normalization are described in [12], however, a higher indicator value means a more informative and richer test in terms of strain heterogeneity.

Table 1. Absolute and relative weights for the adjustment and normalization of the indicator terms.

ω_{a1}	ω_{a2}	ω_{a3}	ω_{a4}	ω_{a5}	ω_{r1}	ω_{r2}	ω_{r3}	ω_{r4}	ω_{r5}
1	4	0.25	1	1	0.3	0.03	0.17	0.4	0.1

In a similar way, the scalar indicator proposed by Barroqueiro et. al. [7] is used to evaluate the stress states heterogeneity, in this case, considering only tension, compression, and shear. It can be stated as

$$id = \prod_{s=1}^3 \left[\frac{3}{\sum_{e=1}^n X_e} \sum_{e=1}^n (\delta_e^s Z_e X_e) \right]. \quad (2)$$

The index s relates to the stress state, compression, shear, and tension, respectively. The term Z_e stands for the penalization of stress concentrations and unstressed material while the parameter δ_e^s is responsible for identifying the stress state in each element e . In this case, the term X_e corresponds to the volume of each finite element. The ideal solution would present the same amount of material in the three stress states (tension, compression, and shear) without stress concentrations or unstressed material. The multiplicative behavior of the indicator leads to values close to zero most the elements are subjected to tensile loading, being only a few subjected to shear and compression. More information on the computation of the indicator can be found in [7].

Another metric, proposed by Oliveira et. al. [18], evaluates the sensitivity of the test to anisotropy. It was derived from Mohr's circle equations, and it was introduced for a plane stress state. Based on the principal angle's formulation, it considers the maximum principal stress in absolute value, and the range of tensile orientations typically used to calibrate the material's anisotropic behavior. Represented by γ and denominated by rotation angle, it refers to the principal direction associated with the maximum principal stress in absolute value and, it ranges from 0° and 90° , being given by

$$\gamma = \begin{cases} 45 & \text{if } \sigma_{xx} = \sigma_{yy} \text{ and } \sigma_{xy} \neq 0 \\ 45(1 - q) + q|\beta| & \text{otherwise} \end{cases} \quad (3)$$

where β is the principal angle and q is an integer that ranges between -1 and 1 , that can be defined as

$$q = \frac{\sigma_{xx} - \sigma_{yy}}{|\sigma_{xx} - \sigma_{yy}|} \frac{|\sigma_1| - |\sigma_2|}{||\sigma_1| - |\sigma_2||} \quad (4)$$

where σ_1 and σ_2 are the principal major and minor stresses, respectively. Since a rotation angle value is related to each material point, an average metric needs to be defined to characterize the sensitivity to anisotropy of each test. Therefore, it is proposed to use the standard deviation measure of the rotation angle to evaluate each test.

Specimen designs. In this work, three specimen designs proposed in the literature were chosen to be analyzed. To improve the quality of the information that can be extracted from a single mechanical test, their geometries were designed from different approaches. The first design was proposed by Rossi et. al. [19] and is usually referenced as Notched. Jones et. al. [2] developed the second specimen geometry, referred as D, via an iterative geometry design process aided by engineering intuition. The last specimen was obtained from a topology-based design methodology [20], designed with the goal of presenting the most heterogeneous displacement field. This will be referred to as TopOpt. The selected geometries are depicted in Fig. 1 along with their dimensions. The three specimen geometries were considered to be machined at 45° with respect to the rolling direction (along the x-direction) in order to enhance the heterogeneity of the mechanical fields.

Material behavior. The material considered in this work is a dual-phase steel (DP600) [21] with a thickness of 0.8 mm. The elastic behavior is considered isotropic, being modeled by Hooke's law. The plastic behavior is anisotropic and is defined by the Yld2000-2d anisotropy yield criterion [22]. The isotropic hardening is characterized by the Swift Law. The material parameters that describe the proposed behavior are in Table 2.

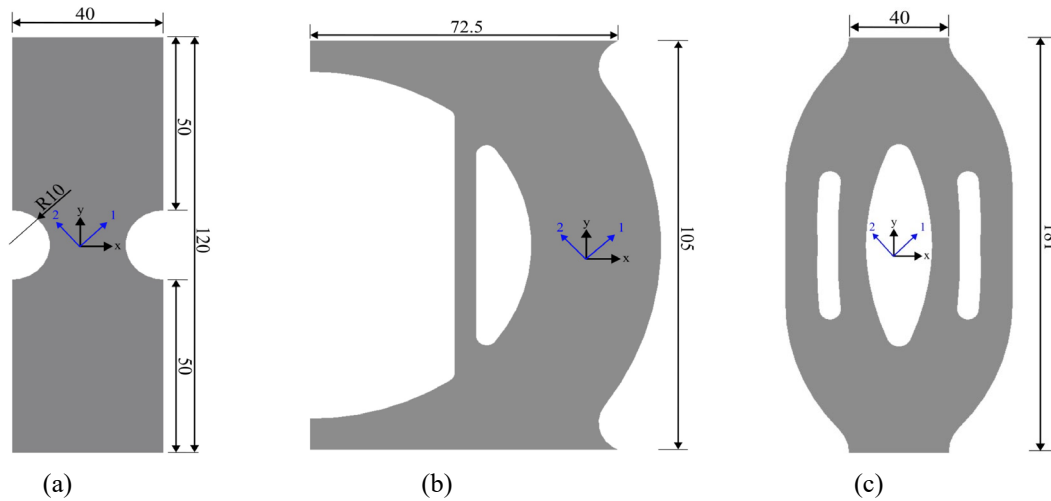


Fig. 1. Specimen designs selected to be analysed in this work: (a) Notched, (b) D and (c) TopOpt.

Table 2. Elastic and constitutive model parameters for the Swift's law and the Yld2000-2d yield function of the DP600 [21].

E [GPa]	ν	K [MPa]	ϵ_0	n					
210	0.3	979.46	0.00535	0.194					
α_1	α_2	α_3	α_4	α_5	α_6	α_7	α_8	a	
1.011	0.964	1.191	0.995	1.010	1.018	0.977	0.935	6	

Numerical simulation. Finite element simulations were carried out using Abaqus/Standard to submit each test configuration to a uniaxial tensile loading. Four-node shell elements were used with reduced integration and hourglass control. An element size of 0.5 mm was used for each specimen. The numerical simulations were performed with automatic time stepping and a maximum increment size of 0.02. The material behavior was described with the aid of a UMMDP (User Material Model Driver for Plasticity). Regarding the boundary conditions of the test, the bottom edge of the specimen was constrained in all degrees of freedom while the displacement at the top edge was constrained in x - and z - directions. A displacement was applied in y - direction. Each mechanical test is performed up to rupture, being the stopping condition established through the Forming Limit Curve (FLC), which is represented in the major and minor strains diagrams of each test. Therefore, the values of the applied displacement that led to rupture were 2.45 mm, 6.38 mm, and 12.45 mm, for the Notched, D and TopOpt, respectively.

Results and Discussion

In this section, the numerical information extracted is used to evaluate the potential of each test. Fig. 2 exhibits the principal stress and strain diagrams and the distribution of the equivalent plastic strain in the specimen just before rupture. Each line stands for the information of one test configuration. The principal strains and stresses diagrams provide huge information on the heterogeneity of the strain and stress fields induced on the specimens as well as the stress and strain state ranges. The equivalent plastic strain distribution on the specimen allows us to understand the areas where a higher magnitude of the variable is achieved. The material points in the elastic regime are represented in grey since these do not provide much information for the characterization of the plastic behavior. By contrast, the color associated with each material point in the plastic regime corresponds to the magnitude of its equivalent plastic strain. All the diagrams present the same scale between tests for easier comparison.

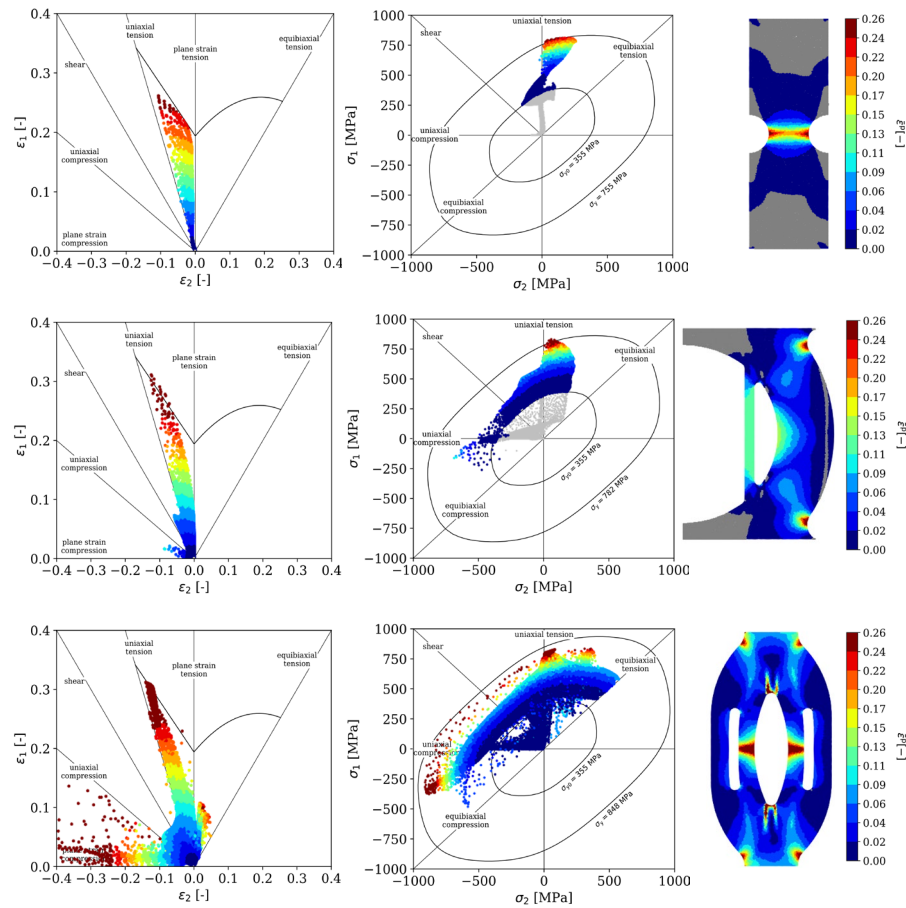


Fig. 2. Principal strains and stresses diagrams and equivalent plastic strain distribution for each test design at the moment just before rupture. Both the initial surface and the one associated with the maximum yield stress are plotted in the principal stress diagrams.

It can be noted that the Notched specimen is the one that presents the smallest stress state range, being limited to uniaxial tension. Similarly, the strain states are mainly located between uniaxial tension and plane strain tension. Regarding the equivalent plastic strain, the higher values of this variable are located in the center part of the specimen. The other material points in the plastic regime are under low values of plastic strain.

In contrast, both D and TopOpt specimens present strain states ranging from plane strain compression and plane strain tension. Although both specimens present material points from uniaxial compression to plane strain compression, the distribution is much denser in the TopOpt specimen. Regarding the principal stresses diagram, there are material points between equibiaxial compression and equibiaxial tension in both specimens, D and TopOpt. However, the latter is the one that presents the largest stress state range. When compared to the Notched specimen, both the D and TopOpt specimens present higher values of plastic strains as well as a larger part of the material points in the plastic regime. In the case of the D specimen, the distribution is more spread, being mainly placed along the curve part of the specimen. The TopOpt specimen presents all the material points in the plastic regime at the moment just before rupture, being the one that achieves higher values of plastic strain. However, these are concentrated in small areas and near the specimen boundaries. This makes the extraction of the information difficult using full-field measurement techniques. It is worth noting that there are material points with plastic strains that are located inside the initial yield surface. This is due to the non-monotonic behavior of some material points. During the test, they enter the plastic regime, but as of a certain point, their strain

paths change direction, leading to a decrease in the induced stresses. Since the equivalent plastic strain consists in a cumulative value, at the moment of rupture, these points are located inside the yield surface but present plastic strains.

With the aim of analyzing quantitatively the information given by the diagrams presented in Fig. 2, the mechanical indicator proposed by [12] has been computed. In Fig. 3, the values of the mechanical indicator for each test configuration are presented as well as its terms individually. All the terms, except for the ones involving the standard deviation computation, were normalized taking into account the size and the number of elements for a fair comparison of the designs.

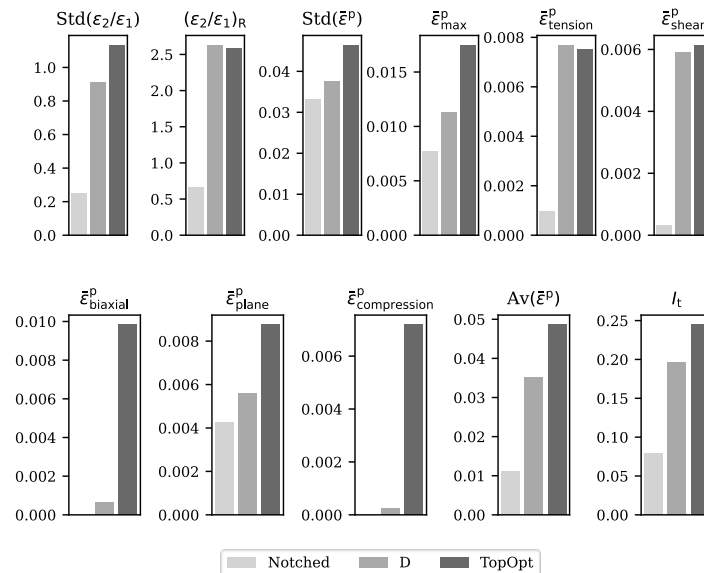


Fig. 3. Values of the mechanical indicator proposed by Souto et. al. [12] and its terms computed individually for all the test designs.

It can be noted that the TopOpt specimen presents the highest overall value of the indicator, followed by the D and the Notched specimens. The higher the indicator value, the more informative the test design is. Regarding the equivalent plastic strain, as has already been referred to previously, the TopOpt presents the highest values and the largest distribution of this variable. It is also the one that presents the most material points in the plastic regime under the strain states evaluated with this indicator. The D specimen also presents an interesting diversity of strain states and equivalent plastic strain distribution. Concerning the strain states range, both specimens present similar performance. Fig. 4 depicts the elements distribution of the D and TopOpt specimens over the strain state range that is limited between -15 and 1. The TopOpt specimen presents a more even distribution of the elements over the presented range although two peaks located around uniaxial tension and between plane strain and uniaxial compression can be noted. In the D specimen, the majority of the material points are between uniaxial tension and shear. Therefore, the standard deviation is higher in the TopOpt specimen than in the D one. However, the second term that evaluates the difference between the maximum and minimum values of the principal strains' ratio is equal for both specimens since these values correspond to the imposed limits. The final value is different due to the normalization of the term concerning the size and number of the elements of each specimen. In previous works [12,23], it was proposed a ranking of the indicator value for well-known standard tests and for new geometries that have been proposed since then. Despite the modification of the strain state range for the computation of the indicator in this work, an updated ranking can be seen in Fig. 5. Also, in the work developed by Thoby et. al [24], it was made a comparison of several specimen designs and this mechanical indicator was used to compare them. Although some terms have been adapted, a similar ranking was obtained.

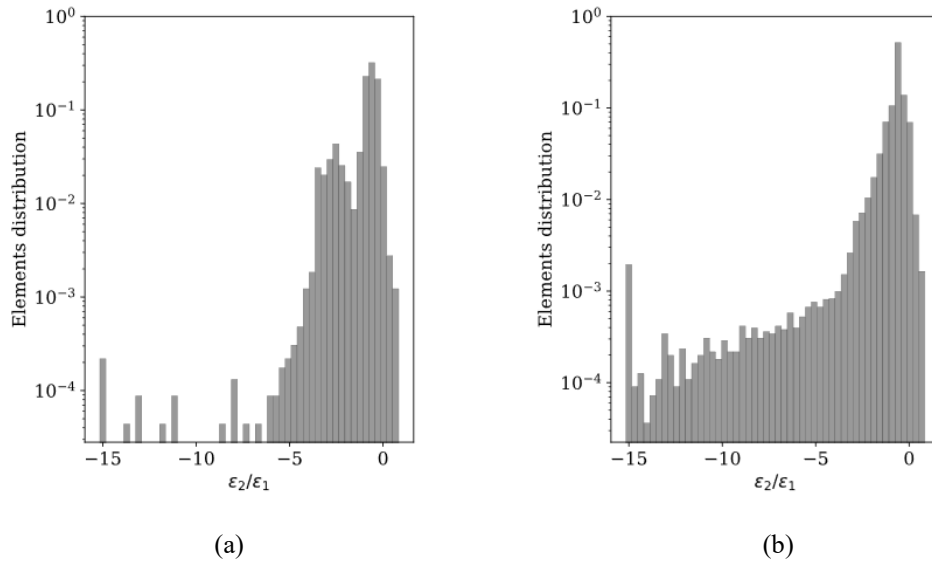


Fig. 4. Elements distribution over the strain state range induced in the (a) D and (b) TopOpt specimens.

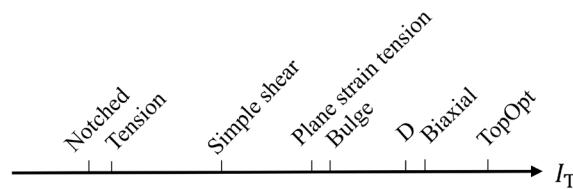


Fig. 5. Ranking for the tests evaluated in [8] and for the Notched, D and TopOpt test designs.

The other mechanical indicator proposed to evaluate the performance of the specimens is the one proposed by [7]. Fig.6 provides the value of the indicator as well as the terms corresponding to each stress state analyzed. Overall, the TopOpt specimen is the one that presents the highest heterogeneity of stress states (tension, compression, and shear). It can be noted that the stress states under which all the specimens present more material points is tension, followed by shear. In compression, there is a significant difference between the TopOpt and the others. The TopOpt specimen was designed considering this indicator, so it is expected that this design presents the highest value.

The rotation angle provides information on the sensitivity of the test to anisotropy. Fig. 7 represents the distribution of the material points over the range of rotation angle values (0° to 90°) for each test configuration. The more dispersed the distribution, the higher the sensitivity to the anisotropic behavior it presents. Therefore, to evaluate quantitatively the information given by the diagrams, it is represented the standard deviation value of the rotation angle of each test design in Table 3. Since the material orientation is 45° in relation to the loading direction, it is expected that most of the material points present rotation angle values in the same order as the material orientation, being the mean value of the rotation angle around 45° for all the test designs. Although the distribution is well dispersed between 0° and 90°, the Notched specimen is the test with the lowest standard deviation value, presenting the majority of the points in the elastic regime with rotation angle values around 45°. However, there is a significant spread of material points in the plastic regime with rotation angle values between -15° and 75°. In contrast, the D specimen presents most of the material points in the plastic regime between rotation angle values of 30° and 60°. The rotation angle standard deviation of the D specimen is considerably higher than the

Notched one, pointing out the difference between both distributions. The TopOpt specimen presents the best range of rotation angle values, presenting material points in the plastic regime between 0° and 90°, covering the whole range. Although this leads to a lower density of points over the range, it presents the highest standard deviation value of all the tests, allowing us to notice a good sensitivity to anisotropy.

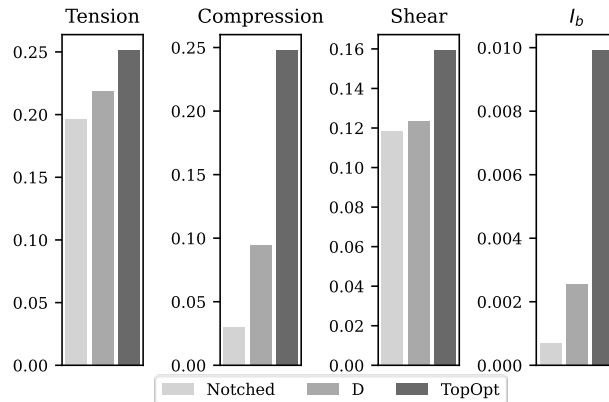


Fig. 6. Values of the performance indicator proposed by Barroqueiro et. al [7] and its terms for all test designs.

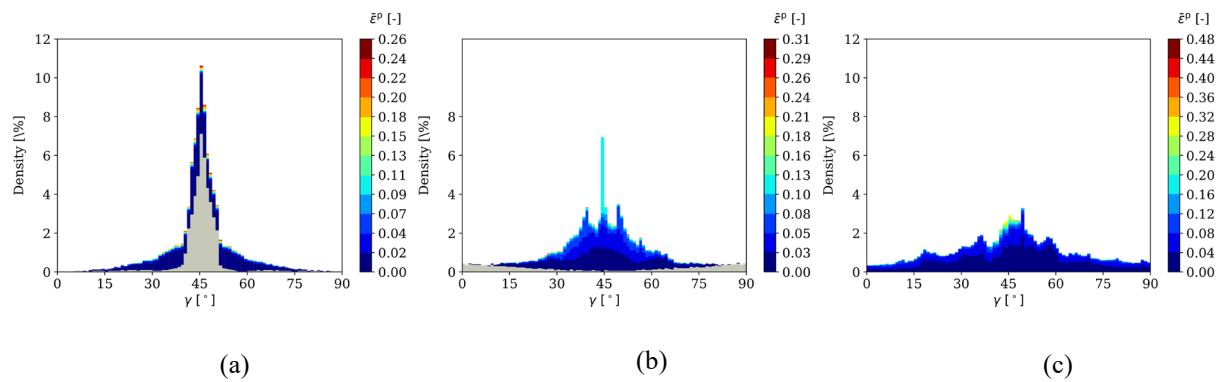


Fig. 7. Rotation angle values for each test configuration: (a) Notched, (b) D and (c) TopOpt.

Table 3. Mean and standard deviation values of the rotation angle distribution for each test design.

	Notched	D	TopOpt
Av(γ) [°]	45.33	44.92	45.70
Std(γ)	10.16	17.38	19.70

Summary

This work aimed at proposing a set of KPIs to evaluate the performance of several test designs in providing the most informative quantity of data for the material behavior characterization and model calibration procedures.

Three specimen designs were subjected numerically to a uniaxial loading test up to rupture. Based on the obtained mechanical fields, the potential of each test design was analyzed and compared with the others. Firstly, the information given by the principal strains and stresses diagrams was quantified by the computation of the mechanical indicator proposed by Souto et. al. [12]. The obtained values allow us to conclude that the TopOpt specimen presented the larger strain state range and most interesting equivalent plastic strain distribution, followed closely by the D specimen. The stress states heterogeneity present in the specimen was also evaluated by the

mechanical indicator proposed by Barroqueiro et. al. [7]. Due to the tensile conditions of the test, all the specimens presented the majority of their material points under tension, being the TopOpt specimen the one with higher heterogeneity of stress states and, therefore, with the higher indicator value. Based on the rotation angle values distribution, it can be concluded that the TopOpt and the D specimens are the ones that present the higher sensitivity to anisotropy due to the higher standard deviation values. Regarding the TopOpt specimen, due to its complex geometry, it may suffer from buckling when tested. However, this situation may lead to a better performance as long as this behavior can be captured by the full-field measurement technique.

This work already consists in a step closer to a more straightforward approach to choose the most informative heterogeneous mechanical test. At this stage, these KPIs evaluate each test based on the diversity of mechanical phenomena and strain and stress states that are covered. However, there is still a need for metrics that take into account the inverse identification quality, for example, the sensitivity of each test to the model parameters and, also, the full-field measurement technique.

Acknowledgments

This project has received funding from the Research Fund for Coal and Steel under grant agreement No 888153. The authors also acknowledge the financial support under the projects UIDB/00481/2020 and UIDP/00481/2020 – FCT – Fundação para a Ciência e Tecnologia; and CENTRO-01-0145-FEDER-022083 – Centro Portugal Regional Operational Programme (Centro2020), under the PORTUGAL 2020 Partnership Agreement through the European Regional Development Fund. M. Gonçalves is grateful to the FCT for the Ph.D. grant Ref. UI/BD/151257/2021.

Disclaimer

The results reflect only the authors' view, and the European Commission is not responsible for any use that may be made of the information it contains.

References

- [1] J.H. Kim, F. Barlat, F. Pierron, M.G. Lee, Determination of Anisotropic Plastic Constitutive Parameters Using the Virtual Fields Method, *Exp. Mech.* 54 (2014) 1189-204. <https://doi.org/10.1007/s11340-014-9879-x>
- [2] E.M.C. Jones, J.D. Carroll, K.N. Karlson, S.L.B. Kramer, R.B. Lehoucq, P.L. Reu, D.Z. Turner, Parameter covariance and non-uniqueness in material model calibration using the Virtual Fields Method, *Comput. Mater. Sci.* 152 (2018) 268-290. <https://doi.org/10.1016/j.commatsci.2018.05.037>
- [3] T. Pottier, P. Vacher, F. Toussaint, H. Louche, T. Coudert, Out-of-plane Testing Procedure for Inverse Identification Purpose: Application in Sheet Metal Plasticity, *Exp. Mech.* 52 (2012) 951–963. <https://doi.org/10.1007/s11340-011-9555-3>
- [4] N. Souto, A. Andrade-Campos, S. Thuillier, Mechanical design of a heterogeneous test for material parameters identification, *Int. J. Mater. Form.* 10 (2016) 353-367. <https://doi.org/10.1007/s12289-016-1284-9>
- [5] M. Conde, Y. Zhang, J. Henriques, S. Coppieters, A. Andrade-Campos, Design and validation of a heterogeneous interior notched specimen for inverse material parameter identification, *Finite Elem. Anal. Des.* 214 (2023) 103866.
- [6] M. Gonçalves, A. Andrade-Campos, B. Barroqueiro, On the design of mechanical heterogeneous specimens using multilevel topology optimization, *Adv. Eng. Softw.* 175 (2023) 103314.
- [7] B. Barroqueiro, A. Andrade-Campos, J. Dias-de-Oliveira, R.A.F. Valente, Design of mechanical heterogeneous specimens using topology optimization, *Int. J. Mech. Sci.* 181 (2020) 105764. <https://doi.org/10.1016/j.ijmecsci.2020.105764>
- [8] P. Wang, F. Pierron, M. Rossi, P. Lava, O.T. Thomsen, Optimised experimental characterisation of polymeric foam material using DIC and the virtual fields method, *Strain* 52 (2016) 59-79.

<https://doi.org/10.1111/str.12170>

- [9] L. Chamoin, C. Jailin, M. Diaz, L. Quesada, Coupling between topology optimization and digital image correlation for the design of specimen dedicated to selected material parameters identification, *Int. J. Solids Struct.* 193-194 (2020) 270-286. <https://doi.org/10.1016/j.ijsolstr.2020.02.032>
- [10] X. Gu, F. Pierron, Towards the design of a new standard for composite stiffness identification, *Compos. Part A Appl. Sci. Manuf.* 91 (2016) 448-460. <https://doi.org/10.1016/j.compositesa.2016.03.026>
- [11] M. Rossi, M. Badaloni, P. Lava, D. Debruyne, F. Pierron, A procedure for specimen optimization applied to material testing in plasticity with the virtual fields method, *AIP Conf. Proc.* 1769 (2016) 200016. <https://doi.org/10.1063/1.4963634>
- [12] N. Souto, S. Thuillier, A. Andrade-Campos, Design of an indicator to characterize and classify mechanical tests for sheet metals, *Int. J. Mech. Sci.* 101-102 (2015) 252-271. <https://doi.org/10.1016/j.ijmecsci.2015.07.026>
- [13] M. Conde, A. Andrade-Campos, M.G. Oliveira, J.M.P. Martins, Design of heterogeneous interior notched specimens for material mechanical characterization, *Esaform 2021, Liège, Belgique, 2021.*
- [14] F. Pierron, M. Grédiac, Towards Material Testing 2.0. A review of test design for identification of constitutive parameters from full-field measurements, *Strain* 57 (2021) 1-22. <https://doi.org/10.1111/str.12370>
- [15] M. Grédiac, The use of full-field measurement methods in composite material characterization: Interest and limitations, *Compos. Part A Appl. Sci. Manuf.* 35 (2004) 751-761. <https://doi.org/10.1016/j.compositesa.2004.01.019>
- [16] S. Avril, M. Bonnet, A.S. Bretelle, M. Grédiac, F. Hild, P. Ienny, F. Latourte, D. Lemosse, S. Pagano, E. Pagnacco, F. Pierron, Overview of identification methods of mechanical parameters based on full-field measurements, *Exp. Mech.* 48 (2008) 381-402. <https://doi.org/10.1007/s11340-008-9148-y>
- [17] F. Pierron, M. Grédiac, *The virtual fields method: Extracting constitutive mechanical parameters from full-field deformation measurements*, Springer Verlag, 2012.
- [18] M.G. Oliveira, S. Thuillier, A. Andrade-Campos, Evaluation of heterogeneous mechanical tests for model calibration of sheet metals, *J. Strain. Anal. Eng. Des.* 57 (2022) 208-224. <https://doi.org/10.1177/03093247211027061>
- [19] M. Rossi, F. Pierron, M. Štamborská, Application of the virtual fields method to large strain anisotropic plasticity, *Int. J. Solids. Struct.* 97-98 (2016) 322-335. <https://doi.org/10.1016/j.ijsolstr.2016.07.015>
- [20] M. Gonçalves, A. Andrade-Campos, S. Thuillier, On the topology design of a mechanical heterogeneous specimen using geometric and material nonlinearities, *IOP Conf. Ser. Mater. Sci. Eng.* 1238 (2022) 012055. <https://doi.org/10.1088/1757-899X/1238/1/012055>
- [21] F. Ozturk, S. Toros, S. Kilic, Effects of Anisotropic Yield Functions on Prediction of Forming Limit Diagrams of DP600 Advanced High Strength Steel, *Procedia Eng.* 81 (2014) 760-765. <https://doi.org/10.1016/j.proeng.2014.10.073>
- [22] F. Barlat, J.C. Brem, J.W. Yoon, K. Chung, R.E. Dick, D.J. Lege, F. Pourboghrat, S.-H. Choi, E. Chu, Plane stress yield function for aluminum alloy sheets - Part 1: Theory, *Int. J. Plast.* 19 (2003) 1297-1319. [https://doi.org/10.1016/S0749-6419\(02\)00019-0](https://doi.org/10.1016/S0749-6419(02)00019-0)
- [23] J. Aquino, A. Andrade-Campos, J.M.P. Martins, S. Thuillier, Design of heterogeneous mechanical tests: Numerical methodology and experimental validation, *Strain* 55 (2019) 1-18. <https://doi.org/10.1111/str.12313>
- [24] J.D. Thoby, T. Fourest, B. Langrand, D. Notta-Cuvier, E. Markiewicz, Robustness of specimen design criteria for identification of anisotropic mechanical behaviour from heterogeneous mechanical fields, *Comput. Mater. Sci.* 207 (2022) 111260. <https://doi.org/10.1016/j.commatsci.2022.111260>